OPEN

Postmortem Diffusion-Weighted Magnetic Resonance Imaging of the Brain in Perinatal Death: An Animal Control Study to Detect the Influence of Postmortem Interval

Maud P. M. Tijssen, MD, Simon G. F. Robben, MD, PhD,* Willemijn M. Klein, MD, PhD,† and Paul A. M. Hofman, MD, PhD**

Abstract: Objectives: Diffusion-weighted imaging may be useful as part of a postmortem magnetic resonance imaging protocol. However, apart from the effect of temperature on apparent diffusion coefficient (ADC), normal postmortem ADC changes can influence the interpretation. Therefore, this study was conducted to evaluate the correlation between normal ADC changes and postmortem intervals (PMIs) and develop a reference standard for postmortem changes after temperature correction.

Materials and Methods: Six premature lambs were scanned at different PMIs. ADC values were measured at different parenchymal locations. Correlation and linear regression between ADC values and PMI were analyzed for all locations, both uncorrected and corrected for temperature.

Results: All locations showed a significant negative correlation between the PMI and ADC value, with (R^2 = 0.581–0.837, $P < 0.001$) and without (R^2 = 0.183–0.555, $P < 0.001$–0.018) temperature correction.

Conclusions: The postmortem interval is negatively correlated with ADC values in the brain. A correlation coefficient for the PMI can be calculated after temperature correction to predict ADC changes. However, further research is required to evaluate its clinical application in humans.

Keywords: autopsy, diffusion-weighted imaging, fetus, magnetic resonance imaging, postmortem changes

(*Top Magn Reson Imaging* 2022;31:43–50)

The use of postmortem magnetic resonance imaging (PMMRI) as an adjunct or a replacement of conventional autopsy has been increasing,[1,2] with a significantly higher parental acceptance rate of PMMRI as a noninvasive or minimally invasive procedure compared with that of conventional autopsy.[3–6] However, PMMRI has several limitations, mainly associated with low birth weight and autolytic and maceration changes.[7–9]

T2-weighted imaging is considered as the most important sequence for PMMRI.[10,11] However, the use of diffusion-weighted imaging (DWI) remains debatable. The efficacy of DWI in detecting postischemic damage and other neurological disorders in vivo is well established. This raises the question whether DWI is helpful in PMMRI as well because DWI changes are also dependent on the degree of normal postmortem processes (eg, maceration, autolysis, and postmortem interval [PMI]) and temperature.[12–16] These factors make the differentiation between the normal and expected postmortem apparent diffusion coefficient (ADC) changes and the pathological changes challenging.

Normal postmortem ADC changes are time dependent. This has also been evaluated in adults.[17] The course of ADC changes in fetuses and neonates is quite different from that in adults, probably because of the different composition of the parenchyma, especially the myelination degree.[18–20] If normal postmortem ADC changes can be predicted, DWI can be used to detect abnormal (premortem) changes. A reference standard created for ADC changes correlated with postmortem intervals (PMIs) can enhance the potential use of DWI to detect pathological changes in neonatal death. This study evaluated the ADC changes in the first 24 hours, corrected for temperature-dependent ADC changes, to detect the possibility of creating a reference standard for normal changes correlated with PMI in the nonmyelinated brains of lambs. The body weight and brain volume of lambs are nearly comparable with those of neonates.

MATERIALS AND METHODS

Study Cohort

Six prematurely delivered lambs (3 twins) received sequential postmortal imaging over a period of 24 hours of direct postmortem. The lambs were delivered by cesarean section at 130–131 days (which correlates with the gestational age of 35 weeks in humans). Five lambs were sacrificed by intravenous injection of a lethal dose of phenobarbital, administrated 3–6 hours after birth. One lamb (lamb 2) died of natural causes within 4 hours of birth. Demographics, including gestational age, weight (g), and exact age (hours) at the time of death, were recorded. The lambs were scanned postmortem at 5 different time points with a PMI of 2 hours (0.55–2.30 hours), 4 hours (2.50–4.20 hours), 6 hours (4.40–6.25 hours), 16 hours (15–17.20 hours), and 21 hours (20.00–22.00 hours). The bodies were stored at 4°C in between scans.

Magnetic Resonance Imaging Protocol

MR imaging was performed with a 3.0 T (Ingenia CX, Philips Healthcare, Best, the Netherlands) using a 32-channel head coil. Brain imaging included axial T2 sequence and coronal DWI (see Table 1 for MRI pulse sequence parameters). DWI sequences were obtained with diffusion gradient values of b = 500 and b = 1000.

Analysis

Images were imported into a PACS system (IMPAX 6.6.1.5003, Agfa Healthcare N.V., Mortsel, Belgium). Diffusion values were measured by manually placing circular regions of interests on the ADC maps at 6 different locations: frontal white matter (right), basal ganglia (right), right thalamus, pons (midline), right cerebellar hemisphere, and

From the *Department of Radiology, Maastricht University Medical Center, Maastricht, the Netherlands; and †Department of Radiology, Radboud University Medical Center, Nijmegen, the Netherlands.

Received for publication July 4, 2022; revision received August 16, 2022; accepted August 26, 2022.

Address correspondence to Maud P.M. Tijssen, MD, Department of Radiology and Nuclear Medicine, Maastricht University Medical Center, P. Debyelaan 25, P.O. Box 5800, 6202 AZ Maastricht, the Netherlands (e-mail: mpm.tijssen@mumc.nl).

The authors declare no conflicts of interest.

DOI: 10.1097/RMR.0000000000000299

TABLE 1 MRI Pulse Sequence Parameters for the Diffusion-Weighted Images of the Lambs b = 500 and b = 1000 and T2-Weighted Images (axial)

Parameters	DWI (b = 500)	DWI (b = 1000)	T2 (axial)
Echo time (ms)	99	108	80
Repetition time (ms)	6367	6774	5016
FOV (mm)	120 × 118	120 × 118	268 × 168
Acquired resolution (mm^2)	1.00 × 1.02	1.00 × 1.02	0.45 × 0.60
Slice thickness (mm)	1.5	1.5	1.5

DWI indicates diffusion-weighted imaging; FOV, field of view.

vitreous body (right) (Fig. 1). Vitreous body measurements were used for temperature calculations, as explained in the next paragraph. Measurements were performed by a single reader (M.T., >10 years experience), with the same measurements performed twice for the b500 gradient and twice for the b1000 gradient. The measurements of each b-value were repeated after an interval of more than 1 month from the first measurement in both gradients to minimize intraobserver bias. To evaluate interobserver agreement, a second reader (R.G.C.S., >5 years experience) performed measurements on the b1000 gradient as well. Anatomic correlation was determined by cross-referencing the axial T2-weighted images.

Temperature Calculation

Temperatures were calculated using diffusion-weighted images (b = 1000 values). Kozak et al[15] developed the following formula to calculate the temperature dependence on the diffusion value of cerebrospinal fluid in the ventricle on ADC:

$$T = \frac{2256.74K}{\ln\left[\frac{4392.21\times10^{-3}\frac{mm^2}{s}}{D\frac{mm^2}{s}}\right]} - 273.15K$$

where T is the temperature (°C), D is the diffusion value, and K is Kelvin. Owing to the pre-existent small size and collapse of the ventricles postmortem, the diffusion value of the cerebrospinal fluid in the ventricles could not be reliably measured. Therefore, the diffusion value (D) of the vitreous body was used as an alternative reliable marker.[16] The ADC values of the right eyeball were measured for all lambs at all time points. The temperatures were calculated using these ADC values, and the formula was developed by Kozak et al.[15]

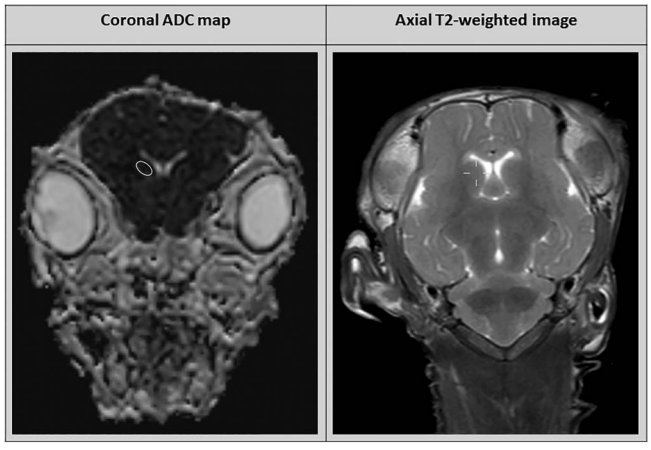

FIGURE 1. Example of ROI placement in a coronal ADC map (b =1000) in the right basal ganglia (left) and axial T2-weighted image for cross-referencing (right). ADC, apparent diffusion coefficient; ROI, regions of interest.

TABLE 2 Example of Temperature Correction of ADC Values in the Basal Ganglia in a Lamb

Scan	Calculated T (°C)	ADC Value (10^{-6} mm^2/s)	Correction Factor	Corrected ADC value (10^{-6} mm^2/s)
1	21.9	334.7	1.52	508.7
2	20.9	323.5	1.56	504.7
3	18.8	292.2	1.65	482.1
4	10.7	174.7	2.06	359.9
5	9.1	150.1	2.15	322.7

Calculated temperature and measured uncorrected ADC values are given in the first 2 columns. By using the formula of Kozak et al, a correction factor for vitreous body is calculated (third column) and extrapolated to the parenchymal region (last column).

ADC indicates apparent diffusion coefficient.

For all time points, an ADC correction ratio to 39°C (normal live temperature in lambs) was calculated by dividing the expected diffusion value (D) at 39°C by the actual measured D in the vitreous body for all time points. The expected D of the vitreous body at 39°C was calculated using the formula described by Kozak et al.[15] The correction ratios were extrapolated to all parenchymal regions, and the corrected ADC values adjusted to a temperature of 39.0°C were calculated (example is presented in Table 2).

Statistical Analysis

Intraobserver bias and agreement were analyzed using the intraclass correlation coefficient and Bland-Altman plots. Intraclass correlation coefficient was also calculated for interobserver agreement. The correlation between ADC values and postmortem intervals for all locations was analyzed. Bivariate regression was conducted to examine the correlation between PMI and ADC values, both uncorrected and corrected for temperature, using SPSS software (IBM SPSS Statistics 25.0). Linear regression analysis assessment of PMI vs. ADC was performed in all 6 different regions using a linear mixed model with STATA version 15.1 (StataCorp LLC, College Station, TX). The predictive margins for all locations with a 95% confidence interval were calculated using a linear mixed model. Statistical significance was defined as $P < 0.05$.

RESULTS

Demographics

The demographic characteristics are presented in Table 3. The weights of the lambs varied between 1400 and 3500 g. The age at the time of death was between 3 hours and 50 minutes and 6 hours and 5 minutes. PMIs at all 5 time points are presented in Table 3.

Intraobserver and Interobserver Variability

The intraobserver correlation was good for all separate parenchymal locations in both b500 and b1000 maps, but better for b1000 than for b500, with a total calculated intraclass correlation coefficient (for parenchymal areas: basal ganglia, frontal white

TABLE 3 Characteristics of the Lambs and PMI at the Time of the Sequential MR Scans

Lamb	Weight (g)	Age at Moment of Death (hours)	PMI Scan 1 (hours)	PMI Scan 2 (hours)	PMI Scan 3 (hours)	PMI Scan 4 (hours)	PMI Scan 5 (hours)
1	2900	3 hours 50 minutes	1 hours 10 minutes	3 hours 25 minutes	5 hours 55 minutes	16 hours 40 minutes	21 hours 40 minutes
2	2700	4 hours 0 minutes	1 hours 45 minutes	3 hours 45 minutes	6 hours 10 minutes	17 hours	22 hours
3	1700	3 hours 50 minutes	2 hours 25 minutes	4 hours 20 minutes	6 hours 25 minutes	16 hours 30 minutes	21 hours 30 minutes
4	1400	6 hours 05 minutes	0 hours 55 minutes	3 hours 10 minutes	4 hours 55 minutes	15 hours 0 minutes	20 hours 0 minutes
5	3500	4 hours 0 minutes	2 hours 30 minutes	4 hours 20 minutes	6 hours 10 minutes	17 hours 20 minutes	21 hours 40 minutes
6	2600	6 hours 0 minutes	1 hours 10 minutes	2 hours 50 minutes	4 hours 40 minutes	15 hours 40 minutes	20 hours 20 minutes

MR indicates magnetic resonance; PMI, postmortem interval.

matter, thalami, pons, and cerebellum) of 0.93 in the b1000 maps and 0.87 in the b500 maps. When calculated for the separate locations, the correlation in all locations on b500 was ≥0.79 (0.79–0.92) and all locations on b1000 was ≥0.90 (0.90–0.96). Bland-Altman plots were created to show the differences between 2 repeated measurements compared with the mean of both measurements (Fig. 2). There was a good correlation between the measurements, and almost all measurements were within the 1.96 standard deviation lines.

Interobserver agreement was good with a total calculated intraclass correlation coefficient of 0.889 ($P < 0.001$) for parenchymal areas. For further interpretation, the mean values of the b1000 maps were used.

ADC Value Versus PMI

A scatterplot showed a statistically significant negative and linear relationship between the ADC value and the PMI in all locations (Fig. 3). This was true for the combined results of all parenchymal areas and for the separate calculations. The R^2 value was lowest in the cerebellum (0.581) and highest in the basal ganglia (0.837). The R^2 value for combined parenchymal locations was 0.676. There were no observational differences between the lamb that died of natural

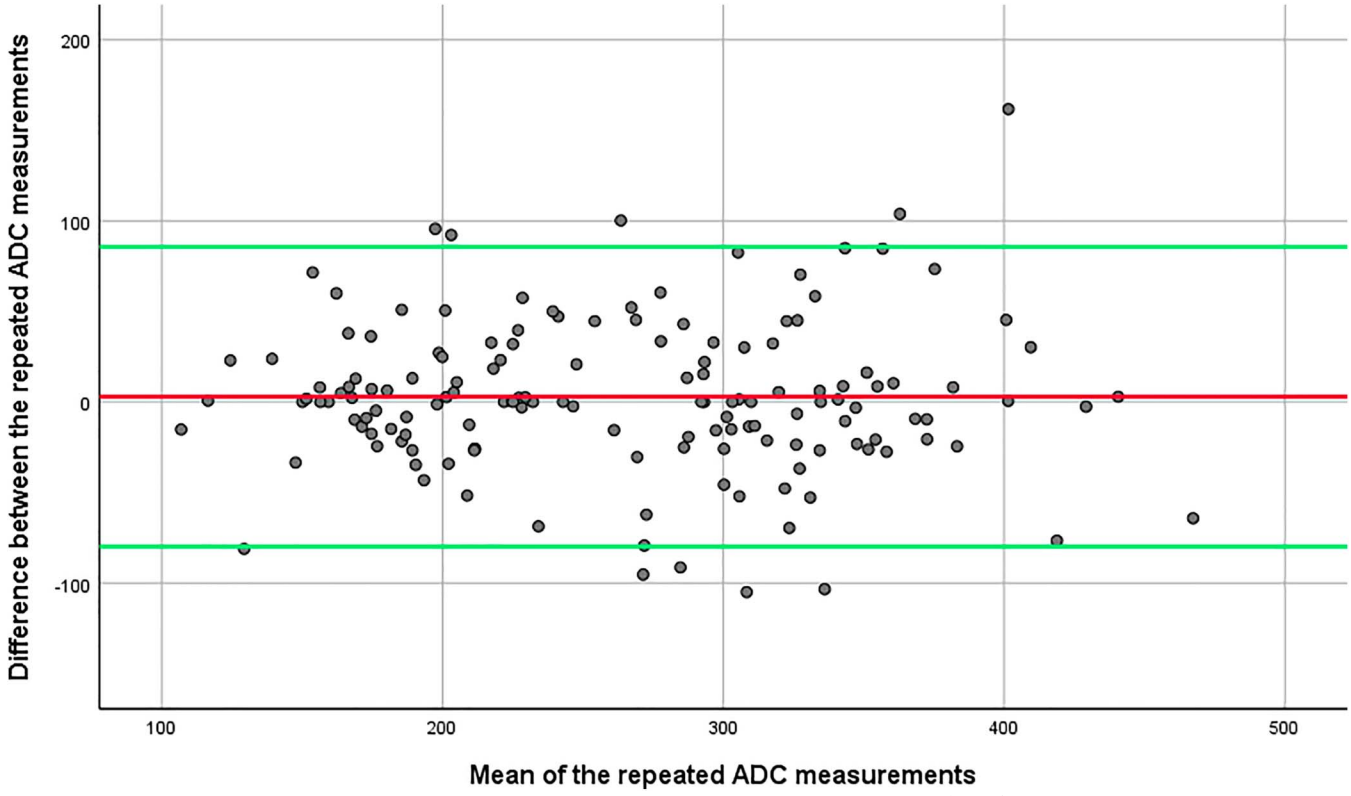

FIGURE 2. Bland-Altman plots of the repeated intraobserver b1000 ADC value measurements (10^{-6} mm^2/s). Red line represents no difference between the 2 measurements; the green lines represent 1.96 SD difference (upper and lower 95% confidence interval) between the measurements. ADC, apparent diffusion coefficient; SD, standard deviation.

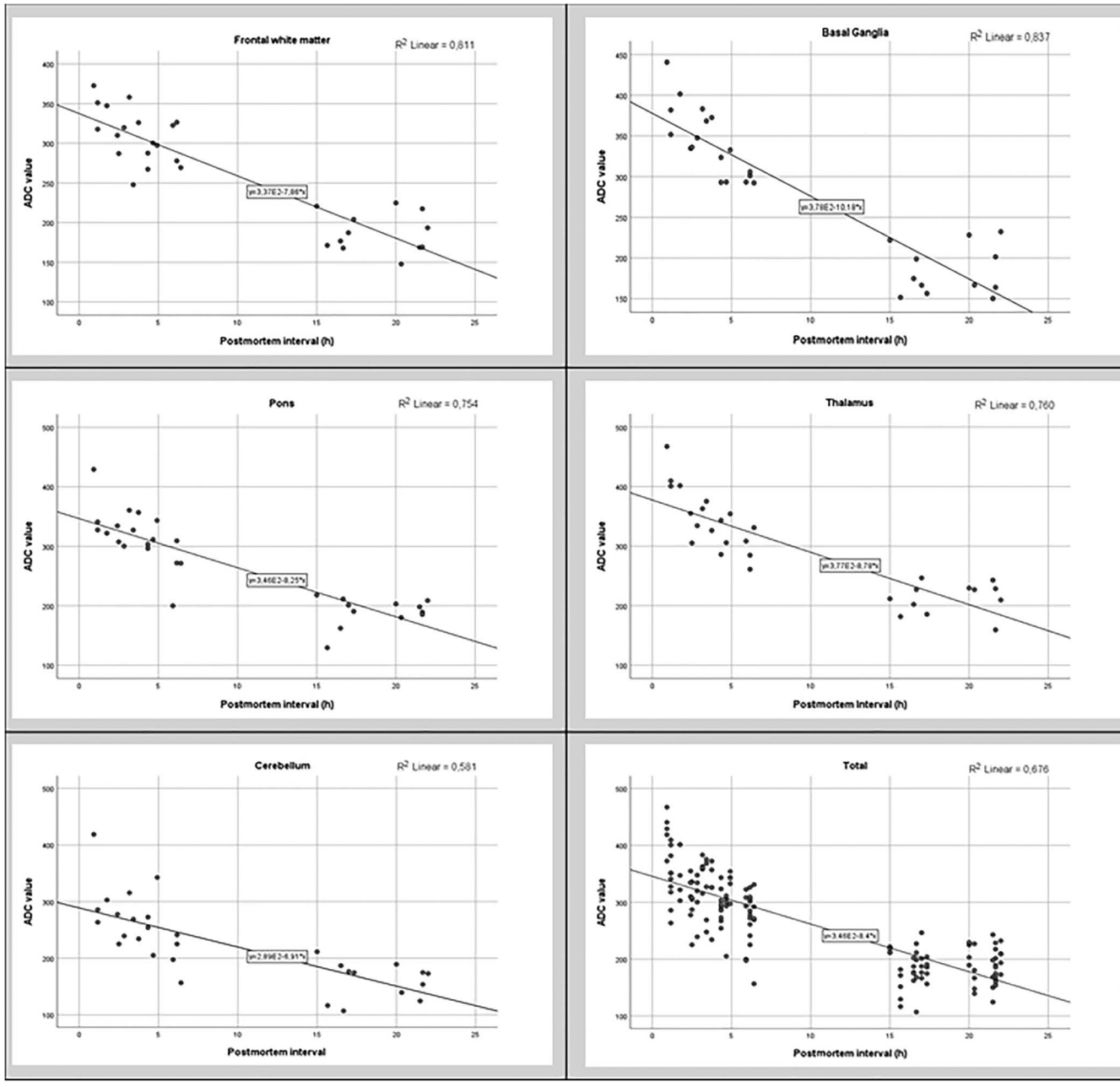

FIGURE 3. Linear regression analysis for the ADC values in the separate and combined parenchymal locations, not corrected for temperature. A negative correlation is shown. ADC, apparent diffusion coefficient.

cause and the lambs that were sacrificed with a lethal dose of phenobarbital.

ADC Value Versus Temperature

The calculated temperature varied between 20.4 and 26.9°C at time point 1 and between 8.4 and 11.9°C at time point 5.

Linear regression was performed after the temperature correction with corrected ADC values adjusted to a temperature of 39.0°C. All parenchymal locations showed a negative correlation between corrected ADC values and PMI (Fig. 4). This was significant in all regions (P values ranging between <0.001 and 0.018). The unstandardized B coefficient (D change per hour [PMI]) calculated for all locations varied between −4.5 (cerebellum) and −8.1 (basal ganglia) (Table 4). Figure 5 illustrates an example of the average course of measured ADC values, corrected and uncorrected, related to the postmortem interval in the frontal white matter in all 6 lambs.

Figure 6 shows the slope of the ADC values at all locations using the linear mixed model. An initial decrease until 15 hours was detected, with a slight increase between 15 and 20 hours at most locations. Compared with time point 1, there was a visible drop in ADC at time point 2, but this was not significant ($P = 0.312$). The further drop at the following time points was significant compared with time point 1 (time point 3, $P = 0.009$; time point 4, $P < 0.001$; and time point 5, $P < 0.001$). Although there was a slight increase at

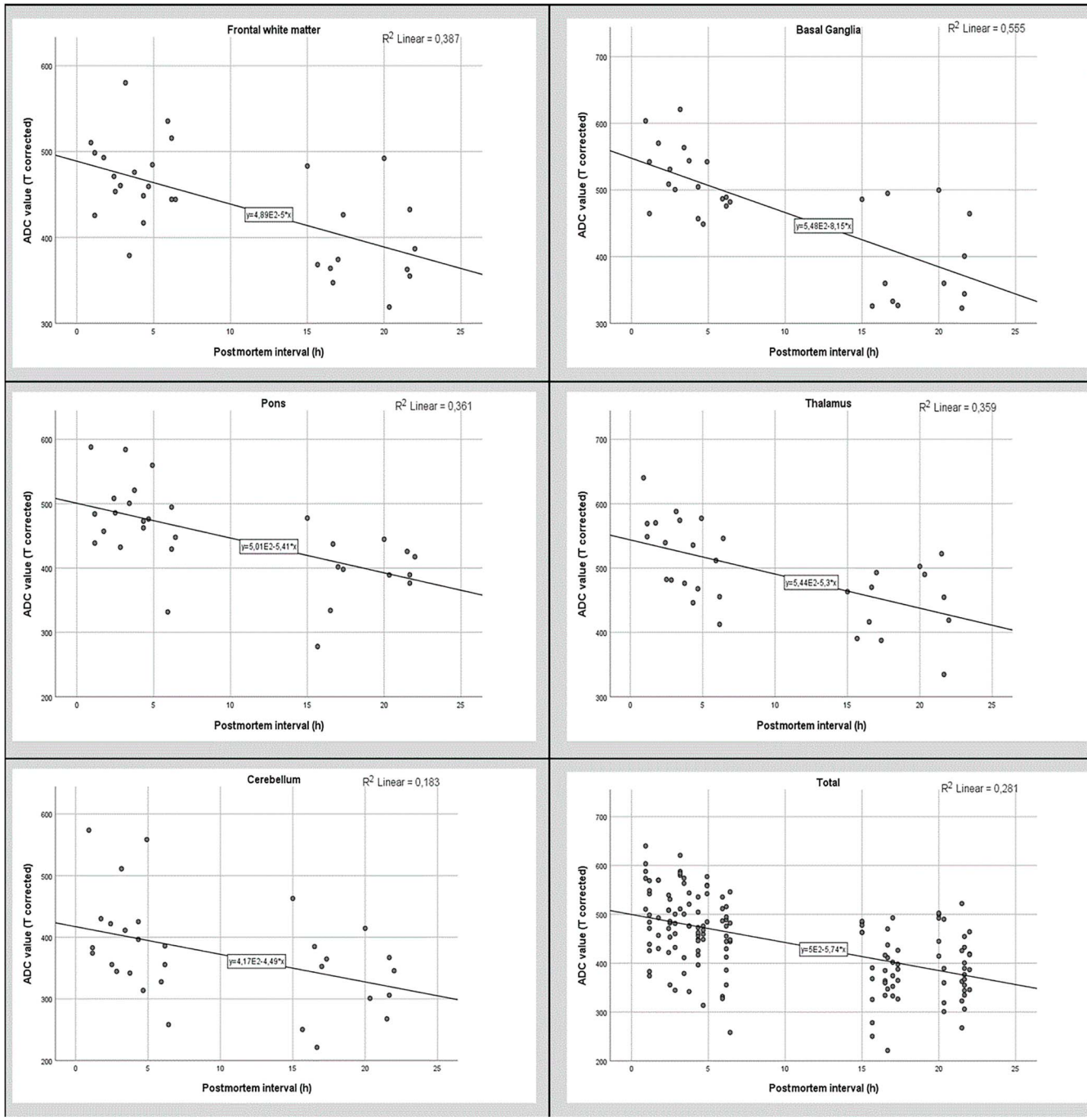

FIGURE 4. Linear regression analysis for the ADC values in the separate and combined parenchymal locations, corrected for temperature. A negative correlation is shown. ADC, apparent diffusion coefficient.

time point 5 compared with time point 4, the total decrease compared with time point 1 was still significant.

DISCUSSION

This study demonstrated a negative correlation between PMI and ADC values in the brain, which persisted after temperature correction of ADC values. Previous studies have shown a decrease in ADC values in postmortem fetuses compared with live fetuses.[21] This decrease in postmortem individuals can be explained by several factors such as maceration, gestational age, temperature, PMI (autolysis), and premortal pathological processes. We evaluated the true effect of PMI on ADC values by excluding or compensating for the following factors that are also associated with the decrease in ADC values.

First, postmortem ADC decrease is highly associated with maceration changes.[12,13] Maceration changes occur after fetal death,

TABLE 4 Correlation Between ADC Values and Postmortem Interval for All Parenchymal Locations and Combined Results

Location	R^2 Without Temperature Correction	*P*	R^2 With Temperature Correction	*P*	Unstandardized B Coefficient
Basal ganglia	0.837	<0.001	0.555	<0.001	−8.148
Frontal white matter	0.811	<0.001	0.387	<0.001	−5.000
Thalamus	0.760	<0.001	0.359	<0.001	−5.304
Pons	0.754	<0.001	0.361	<0.001	−5.405
Cerebellum	0.581	<0.001	0.183	0.018	−4.487
Combined	0.676	<0.001	0.281	<0.001	−5.741

R^2 values for ADC without temperature correction and with temperature correction. There was a negative correlation in all locations, most expressed in the basal ganglia. Unstandardized B coefficient of the ADC value to PMI in the temperature-corrected measurements is given.

ADC indicates apparent diffusion coefficient; PMI, postmortem interval.

with retention of amniotic fluid. In our study, there were no maceration changes as all lambs died postnatally, and no intrauterine fetal death occurred. Therefore, ADC decrease because of maceration changes was excluded from our study.

Second, gestational age has been described as a factor influencing the ADC changes.[12,18–20] In our study, the gestational age was the same in all cases (130–131 days). Therefore, differences in ADC owing to differences in gestational age were also excluded.

Third, our study population consisted of 6 lambs delivered by cesarean section after an uncomplicated pregnancy. Therefore, premortem pathological processes were not expected. This may indicate that changes in ADC are likely the sole effect of normal postmortem changes. When we evaluated the uncorrected ADC values in our study, a decrease was observed, which was significantly correlated with PMI in all regions. However, this drop in ADC values can be attributed to both normal postmortem changes (eg, PMI) and temperature changes, and a correction for the effect of temperature must be made to assess the exact PMI contribution to the ADC decrease. Using the formula provided by Kozak et al,[15] we calculated the temperature in our population at all time points and calculated the correction ratios. Using these ratios, the ADC values were corrected for temperature to filter the effect of PMI on ADC changes.

After temperature correction, a significant negative correlation between ADC and PMI was still visible in all locations, but most significantly in the basal ganglia. The negative correlation between

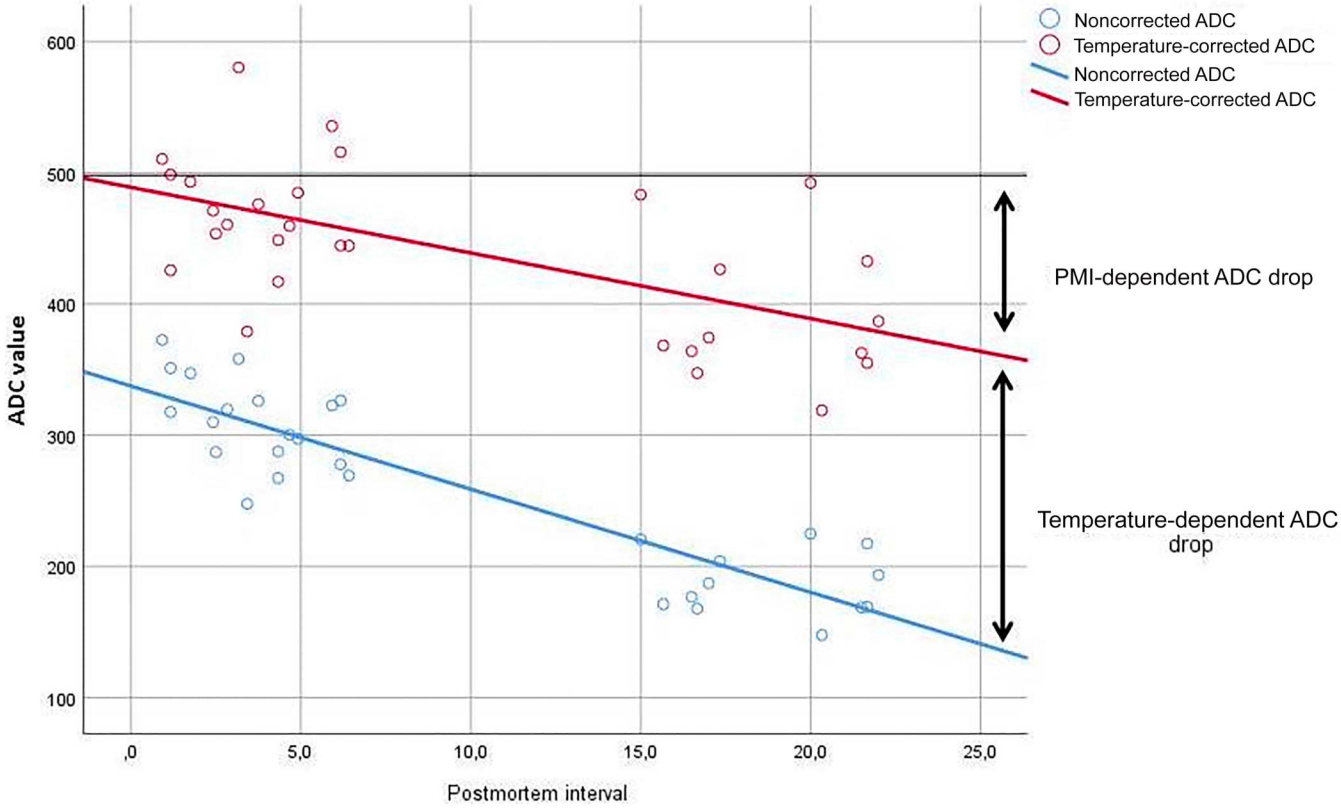

FIGURE 5. Example of the average course of measured ADC values, corrected and uncorrected, related to the postmortem interval in the frontal white matter in all 6 lambs. Temperature-corrected ADC to 39°C is shown in red, and noncorrected ADC course is shown in blue. The blue and red lines represent the average values. A negative correlation is shown in both the corrected and uncorrected measurements. The difference between the red and blue line represents the temperature-dependent ADC drop. The difference between the baseline (black) and red line represents the PMI-dependent ADC drop. ADC, apparent diffusion coefficient; PMI, postmortem interval.

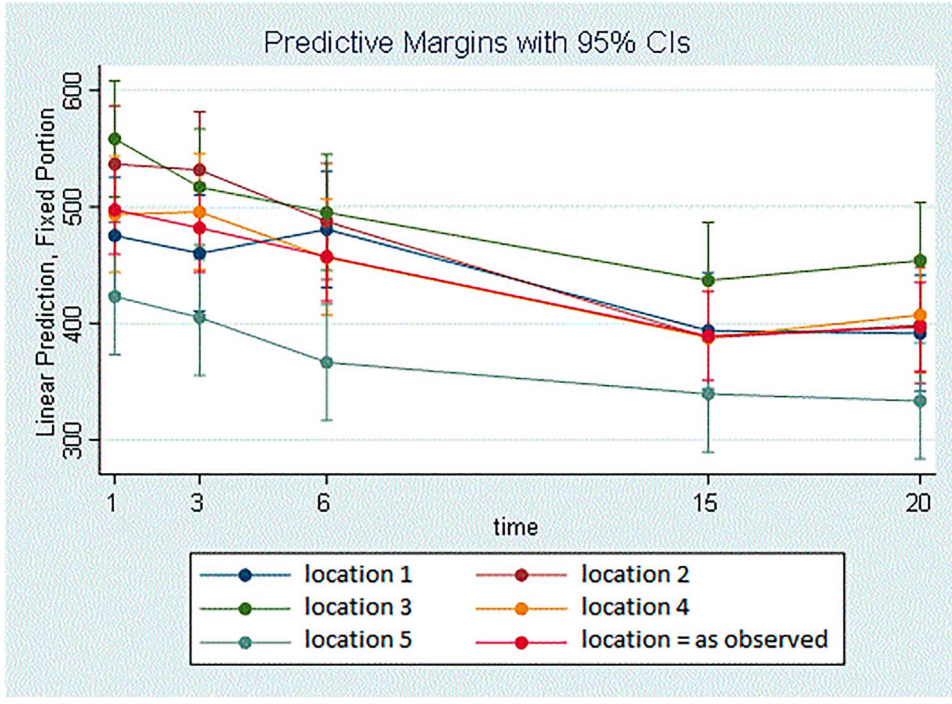

FIGURE 6. Temperature-corrected ADC in all locations: location 1 = frontal white matter, location 2 = basal ganglia, location 3 = thalami, location 4 = pons, and location 5 = cerebellum. An overall negative correlation is shown for all locations dependent on time (postmortem interval). After an initial decrease over the first 15 hours, a slight increase in ADC for the corrected values is shown between 15 and 20 hours. The red line represents the corrected ADC leveled to all 6 lambs and to all 5 locations. ADC, apparent diffusion coefficient; CI, confidence interval.

ADC in the basal ganglia and PMI was also demonstrated by Papadopoulo et al[12]; however, the other parenchymal regions showed no significant negative correlation in this study. Schmidt et al[17] showed an initial increase in ADC until PMI = 5 hours, followed by a decrease until PMI = 19 hours, in an adult population. In our study, this initial increase was not observed even with temperature correction.

The relationship between ADC changes and PMI remains controversial. Several studies have suggested a correlation between the postmortem interval and ADC decrease,[12,14,17] although not confirmed in all regions, and with the overriding effect of maceration change. Shelmerdine et al[13] showed no relationship between PMI and ADC; however, the ADC was evaluated in the body and not in the brain. Arthurs et al[22] showed an increase in ADC in the lungs but did not evaluate brain regions.

Our study had several limitations. First, it was an animal study. Although the trend of PMI on ADC changes is likely the same in humans, the results cannot be fully extrapolated to human fetuses. Second, the study population was relatively small. Although 30 different time points were evaluated, this was based on a population of 6 lambs. To validate this method, studies with larger populations are necessary to correct for individual variation. Third, we studied the effect of PMI on ADC in the first 24 hours. However, owing to the study logistics, we did not continue to scan during the night; therefore, there is an interval between the first 3 scans (2-4-6 hours) and the last 2 scans (16–21 hours). In clinical situations, PMMRI is often performed after 24 hours. Therefore, before its clinical use, this method should be tested in human populations with underlying pathological processes and the effect after 24 hours must be evaluated.

We used corrected ADC values obtained from correction ratios calculated by measuring the ADC values in the vitreous body. When validated with this method, an algorithm can be formulated to predict normal ADC changes because of temperature drop and increasing PMI to further extract the possible pathological ADC decrease to evaluate the underlying pathological processes.

CONCLUSION

ADC values in the brain are negatively correlated with the PMI. A correlation coefficient for the PMI can be calculated after temperature correction to predict physiological ADC changes; hence, moving forward to evaluate possible pathological ADC changes in the future. Further research in a human population with larger study populations and longer PMIs is needed to validate this method.

ACKNOWLEDGMENTS

Remco G.C. Santegoeds, MD, PhD, Department of Radiology, Maastricht University Medical Center, Maastricht, The Netherlands as second reader.

REFERENCES

1. Addison S, Arthurs OJ, Thayyil S. Post-mortem MRI as an alternative to non-forensic autopsy in foetuses and children: from research into clinical practice. *Br J Radiol*. 2014;87:20130621.
2. Thayyil S, Sebire NJ, Chitty LS, et al. Post-mortem MRI versus conventional autopsy in fetuses and children: a prospective validation study. *Lancet*. 2013; 382:223–233.
3. Shruthi M, Gupta N, Jana M, et al. Comparative study of conventional and virtual autopsy using postmortem MRI in the phenotypic characterization of stillbirths and malformed fetuses. *Ultrasound Obstet Gynecol*. 2018;51: 236–245.

4. Cannie M, Votino C, Moerman P, et al. Acceptance, reliability and confidence of diagnosis of fetal and neonatal virtuopsy compared with conventional autopsy: a prospective study. *Ultrasound Obstet Gynecol*. 2012;39:659–665.
5. Ben-Sasi K, Chitty LS, Franck LS, et al. Acceptability of a minimally invasive perinatal/paediatric autopsy: healthcare professionals' views and implications for practice. *Prenat Diagn*. 2013;33:307–312.
6. Kang X, Cos T, Guizani M, et al. Parental acceptance of minimally invasive fetal and neonatal autopsy compared with conventional autopsy. *Prenat Diagn*. 2014;34:1106–1110.
7. Arthurs OJ, Hutchinson JC, Sebire NJ. Current issues in postmortem imaging of perinatal and forensic childhood deaths. *Forensic Sci Med Pathol*. 2017;13:58–66.
8. Jawad N, Sebire NJ, Wade A, et al. Body weight lower limits of fetal postmortem MRI at 1.5 T. *Ultrasound Obstet Gynecol*. 2016;48:92–97.
9. Thayyil S, Cleary JO, Sebire NJ, et al. Post-mortem examination of human fetuses: a comparison of whole-body high-field MRI at 9.4 T with conventional MRI and invasive autopsy. *Lancet*. 2009;374:467–475.
10. Thayyil S. Less invasive autopsy: an evidenced based approach. *Arch Dis Child*. 2011;96:681–687.
11. Norman W, Jawad N, Jones R, et al. Perinatal and paediatric post-mortem magnetic resonance imaging (PMMR): sequences and technique. *Br J Radiol*. 2016;89:20151028.
12. Papadopoulou I, Langan D, Sebire NJ, et al. Diffusion-weighted post-mortem magnetic resonance imaging of the human fetal brain in situ. *Eur J Radiol*. 2016;85:1167–1173.
13. Shelmerdine SC, Main C, Hutchinson JC, et al. The use of whole body diffusion-weighted post-mortem magnetic resonance imaging in timing of perinatal deaths. *Int J Legal Med*. 2018;132:1735–1741.
14. Scheurer E, Lovblad KO, Kreis R, et al. Forensic application of postmortem diffusion-weighted and diffusion tensor MR imaging of the human brain in situ. *AJNR Am J Neuroradiol*. 2011;32:1518–1524.
15. Kozak LR, Bango M, Szabo M, et al. Using diffusion MRI for measuring the temperature of cerebrospinal fluid within the lateral ventricles. *Acta Paediatr*. 2010;99:237–243.
16. Tijssen MPM, Hofman PAM, Robben SGF. Postmortem fetal temperature estimation with magnetic resonance imaging: apparent diffusion coefficient measurements in the vitreous body and cerebrospinal fluid. *TMRI*. 2022;31:25–30.
17. Schmidt TM, Fischer R, Acar S, et al. DWI of the brain: postmortal DWI of the brain in comparison with in vivo data. *Forensic Sci Int*. 2012;220:180–183.
18. Tarui T, Khwaja OS, Estroff JA, et al. Fetal MR imaging evidence of prolonged apparent diffusion coefficient decrease in fetal death. *AJNR Am J Neuroradiol*. 2011;32:E126–E128.
19. Cannie M, De Keyzer F, Meersschaert J, et al. A diffusion-weighted template for gestational age-related apparent diffusion coefficient values in the developing fetal brain. *Ultrasound Obstet Gynecol*. 2007;30:318–324.
20. Boyer AC, Goncalves LF, Lee W, et al. Magnetic resonance diffusion-weighted imaging: reproducibility of regional apparent diffusion coefficients for the normal fetal brain. *Ultrasound Obstet Gynecol*. 2013;41:190–197.
21. Paternoster M, Perrino M, Travaglino A, et al. Parameters for estimating the time of death at perinatal autopsy of stillborn fetuses: a systematic review. *Int J Legal Med*. 2019;133:483–489.
22. Arthurs OJ, Price GC, Carmichael DW, et al. Diffusion-weighted perinatal postmortem magnetic resonance imaging as a marker of postmortem interval. *Eur Radiol*. 2015;25:1399–1406.